Supplemental Information

Materials and Methods

Plasmid Construction, Generation of Transgenic plants

Constructs for mating-based split-ubiquitin and FRET-FLIM assays were generated using Gateway technology (Life Technologies). The constructs of RLP44, BAK1 and BRI1 in pMetYC-Dest and pXNubA22-Dest were already described (1). BAK1-HA was generated by recombination of the available BAK1 entry clone (1) with pGWB14 using Gateway technology. Similarly, BRI1-GFP was created using pH7FWG2 (2). The pRLP44-GFP-GUS lines were created using primers RLP44prom_GW_L and RLP44prom_GW_R and destination vector pKGWFS7 (2). PSKR1-GFP was already described in Ladwig et al., 2015 (3). For the FRET-FLIM assays with RLP44 and BRI1, the destination vector pFRETtv-2in1-CC was used (4). For this system, the respective genes had to be cloned into pDONR221 P1P4 and pDONR221 P3P2 using multisite Gateway technology (Life Technologies). FLS2 (at5g46330) ORF was amplified from plasmid DNA under omission of the stop codon with forward primer FLS2_attB1_F and reverse primer FLS2_attB4_R. RLP44 was amplified with RLP44_attb3_F and RLP44_attb2_R omitting the stop codon and BRI1 was amplified with primers BRI1_attB3_F and BRI1_attB2_R. Subsequently, the respective constructs were cloned into the pFRETtv-2in1-CC. We generated the 2in1 constructs RLP44-mTurquoise-FLS2-mVenus and RLP44-mTurquise-BRI1-mVenus. Oligonucleotides are described in Table S1.
All other constructs are based on the GreenGate system (5). For details regarding cloning and constructs please see Table S2. For BRI1 (at4g39400) CDS GreenGate Cloning, three internal BsaI/Eco31I recognition sites were removed through the generation of 4 PCR fragments with following primers BRI1_GGC_1F, BRI1_GGC_1R, BRI1_GGC_2F BRI1_GGC_2R, BRI1_GGC_3F, BRI1_GGC_3R, BRI1_GGC_4F and BRI1_GGC_4R. Subsequently the PCR products of all combinations were gel purified, digested with Eco31I, ligated and continued according to the GreenGate protocol (5).

Genotyping

For genotyping of the *bri1-null* T-DNA insertion line, we used for the wildtype allele BRI1-GK_WT_F and primer BRI1_3'UTR_R. Presence of the T-DNA insertion was assessed with primers GK-o8409 and BRI1_GK-134E10_R. The presence of the *bri1-116* allele in segregating *bri triple* and 35SRLP44-GFP (*bri triple*) seedlings was determined with primers bri1-116_CAPS_F and bri1-116_CAPS_R and subsequent digestion of the PCR product with MssI. For *pskr1-3* mutants, primers SALK_008585_F and SALK_008585_R were used to detect the wildtype allele and primers SALK_008585_F and LBb1.3 were used to detect the T-DNA. For *pskr2-1* mutant, SALK_203857_F and SALK_203857_R were combined for the wildtype allele and SALK_203857_F and LBb1.3 for the T-DNA. Genotyping of *rlp44*^{cnu2} is described in (1).

Analysis of Xylem and Total Vascular Cell Number

For Basic Fuchsin staining, 6 day old seedlings were fixed in methanol for 1-2 hours using 6-well plates with cell strainers and subsequently placed in 10% (w/v) NaOH and incubated for 3-4 hours at 65°C. After removal of the NaOH solution, seedlings were stained in 0.01% basic fuchsin (w/v) in water for five minutes, destained in 70% (v/v) ethanol for 10 minutes, and stored in 50% (v/v) glycerol. Samples were mounted in 50% Glycerol and imaged on a Zeiss LSM 510 or a Leica SP5 using excitation of 514 nm. Fluorescence emission was detected with

a 560 nm long pass filter. Xylem cell type was determined via the patterning of ligninified secondary cell all thickenings from z stacks. For Calcofluor White staining of the cell walls, seedlings were placed in 1 M KOH solution for 6 hours at 37°C. After removal of KOH, seedlings were washed three times in 50 mM Tris-HCl pH 7.5, and with 100 µg/µl Calcofluor white in the same buffer for 1.5 hours on a benchtop shaker. After three washing steps with 50 mM Tris-HCL pH7.5, seedlings were stored in 50% glycerol. Samples were mounted in 50% Glycerol and imaged on a Zeiss LSM 510 using excitation at 405 nm and detection with a 420-480 nm band pass filter.

Immunoprecipitation and Western Blotting

Transient expression was performed in leafs of 4-6 week old *Nicotiana benthamiana* plants through Agrobacteria infiltration (OD_{600} = 1). Two days after transformation, 0,75 g plant material was harvested. PSK was infiltrated 60 min before harvesting. For immunoprecipitation from Arabidopsis, 6 to 9 day old seedlings grown on plates as described were harvested, and up to 1 g plant material was frozen in liquid nitrogen. The following steps were the same for both experimental approaches. The plant material was ground using 2 ml/g of extraction buffer (50mM Tris-HCL pH 7.5, 150 mM NaCl, 10% glycerol, 5 mM EDTA, 1% NP40, 5 mM DTT and 1 % plant protease inhibitor cocktail). The total ground material was spun down for 15 min in a table top centrifuge (max. rpm, 4 °C). 60 µl of the protein extract was taken as the input sample and boiled with 20 µl of 4x SDS-PAGE sample buffer (Roti Load1, Roth) at 95 °C. The remaining protein extract was incubated with GFP-trap or RFP-trap agarose beads. For each sample, 30 µl of beads were equilibrated in 1 ml of the extraction buffer and spun down for 5 min in centrifuge (500 rpm, 4°C). After removal of the supernatant, the protein extract was added to the beads and incubated for 2 hours at 4°C (over-head shaker). After incubation, the beads were washed three times with extraction buffer and the supernatant was discarded. The remaining beads were boiled in 60 µl of 2x SDS-PAGE sample buffer at 95 °C for 5 min. SDS-PAGE gels were self-prepared and for RLP44 detection 12% gels, for BAK1 10% and for BRI1 6 or 7 % gels were used. The same protein quantity was loaded in the SDS-PAGE and after Western blotting probed with the indicated antibodies. Before probing with the antibodies the PVDF membrane (Immobilon-P, Millipore) was blocked for 1 h in 5% BSA in 1 x TBST blocking solution (20 nM Tris-base pH 7.4, 150 mM NaCl, 0.05% Tween). Primary antibodies, mouse anti-GFP (1GFP63, Biolegend, 1:10000), mouse anti-HA (F-7, Santa Cruz Biotechnology, 1:5000), rabbit anti-RFP (1:10000), rabbit anti-BRI1 ((6), 1:5000) and rabbit anti-BAK1 ((6), 1:10000) were diluted in 3 % BSA and incubated with the membrane overnight at 4 °C on a shaker. Membranes were washed 8 x 5 min with 1 X TBST before they were incubated with the secondary antibodies, goat polyclonal anti-rabbit coupled to horseradish peroxidase (Thermo Fisher Scientific, 1:10000) or rabbit polyclonal anti-mouse coupled to horseradish peroxidase (Sigma-Aldrich, 1:10000) diluted in in 3% BSA for 1 hour on gentle agitation on room temperature. Membranes were again washed 8 x 5 min before imaging with an INTAS science imaging device using a chemiluminescence detection kit (Supersignal West Pico, Thermo Fischer Scientific).

Quantitative Reverse Transcription PCR

Total RNA was extracted from roots of 5 day old seedlings. Not more than 100 mg of roots were frozen in liquid nitrogen and RNA was extracted with the GeneMATRIX Universal RNA Purification Kit (EURx/Roboklon) with an additional DNaseI digestion step, either directly on the column (Roboklon DnaseI-RNase free E1345) or subsequently DNase I digestion (DNase I, RNase-free, Thermo Fisher Scientific EN0525) followed by a RNA column clean-up (Roboklon RNA Purification Kit). 1 µg RNA in 5,75 µL RNase free water was used for cDNA synthesis with AMV Reverse Transcriptase Native according the manufacturer's protocol (Roboklon E1372) with RiboLock RNase Inhibitor (Thermo Fisher Scientific EO0381). qPCR reactions were performed in 15 µL volume, of which are 5 µL 1:40 diluted cDNA template in water, 0.3 µL of JumpStartTM Tag DNA Polymerase (Sigma-Aldrich), 1.5 µL appropriate

buffer, 0.3 µM of each forward and reverse primer, 2 µM dNTPs (Sigma-Aldrich), 0.6 mM $MgCl_2$ and 0.15 µL of 1:400 diluted SYBR ® Green I (Sigma-Aldrich) and fill up with H_2O. Gene expression was normalized to housekeeping gene clathrin adaptor subunit (7). Primer sequences are listed in the table. Ct values were measured in the Rotor Gene Q 2plex (Qiagen) and the data was analysed with the 75 Rotor-Gene Q 2plex software and evaluated according to (8) and (9).

Confocal Laser-Scanning Microscopy

Laser lines of 405 nm (Calcofluor White), 488 nm (GFP, FM4-64), 514 nm (YFP, basic fuchsin), or 543 nm (RFP, mCherry, propidium iodide) on a Zeiss LSM 510 Meta and Leica SP5 microscope systems equipped with 25× and 63× water immersion objectives were used for excitation. Fluorescence was recorded between 420 and 480 nm for Calcofluor White, between 530 and 600 nm for YFP, and between 490 and 525 nm for GFP. FM4-64 fluorescence was recorded between 600 nm and 720 nm and propidium iodide was recorded using a 560 nm long pass filter. Images were analyzed with Zeiss Zen software and Fiji. Images were processed with Fiji and Adobe Photoshop CS for figure preparation.

Mating-Based Split-Ubiquitin Assay and FRET-FLIM Analysis

mbSUS and FRET-FLIM were performed as described (1, 10).

Glucuronidase staining

GUS staining was performed as described (11).

Statistical Analysis

The number of samples analyzed for quantifications are indicated in the figures as (n). The significance of difference between samples were determined by One-way ANOVA combined with Tukey's post hoc test, or by Student's t-test. Xylem cell numbers were analyzed using Mann-Whitney U-test or Kruskal-Wallis modified U-test and Dunn's post hoc test with Benjamini-Hochberg correction. QRT-PCR was analysed as described (9), followed by one-way ANOVA.

References

1. Wolf S*, et al.* (2014) A receptor-like protein mediates the response to pectin modification by activating brassinosteroid signaling. *Proc Natl Acad Sci U S A* 111(42):15261-15266.
2. Karimi M, Inze D, & Depicker A (2002) GATEWAY vectors for Agrobacterium-mediated plant transformation. *Trends Plant Sci* 7(5):193-195.
3. Ladwig F*, et al.* (2015) Phytosulfokine Regulates Growth in Arabidopsis through a Response Module at the Plasma Membrane That Includes CYCLIC NUCLEOTIDE-GATED CHANNEL17, H+-ATPase, and BAK1. *Plant Cell* 27(6):1718-1729.
4. Hecker A*, et al.* (2015) Binary 2in1 Vectors Improve in Planta (Co)localization and Dynamic Protein Interaction Studies. *Plant Physiol* 168(3):776-787.
5. Lampropoulos A*, et al.* (2013) GreenGate---a novel, versatile, and efficient cloning system for plant transgenesis. *PLoS One* 8(12):e83043.
6. Bojar D*, et al.* (2014) Crystal structures of the phosphorylated BRI1 kinase domain and implications for brassinosteroid signal initiation. *Plant J* 78(1):31-43.

7. Czechowski T, Stitt M, Altmann T, Udvardi MK, & Scheible WR (2005) Genome-wide identification and testing of superior reference genes for transcript normalization in Arabidopsis. *Plant Physiol* 139(1):5-17.
8. Muller PY, Janovjak H, Miserez AR, & Dobbie Z (2002) Processing of gene expression data generated by quantitative real-time RT-PCR. *Biotechniques* 32(6):1372-1374, 1376, 1378-1379.
9. Rieu I & Powers SJ (2009) Real-time quantitative RT-PCR: design, calculations, and statistics. *Plant Cell* 21(4):1031-1033.
10. Grefen C, Obrdlik P, & Harter K (2009) The determination of protein-protein interactions by the mating-based split-ubiquitin system (mbSUS). *Methods Mol Biol* 479:217-233.
11. Wolf S, Mravec J, Greiner S, Mouille G, & Hofte H (2012) Plant cell wall homeostasis is mediated by brassinosteroid feedback signaling. *Curr Biol* 22(18):1732-1737.
12. Wang ZY*, et al.* (2002) Nuclear-localized BZR1 mediates brassinosteroid-induced growth and feedback suppression of brassinosteroid biosynthesis. *Dev Cell* 2(4):505-513.
13. Hruz T*, et al.* (2008) Genevestigator v3: a reference expression database for the meta-analysis of transcriptomes. *Advances in bioinformatics* 2008:420747.
14. Schlereth A*, et al.* (2010) MONOPTEROS controls embryonic root initiation by regulating a mobile transcription factor. *Nature* 464(7290):913-916.
15. Brady SM*, et al.* (2007) A high-resolution root spatiotemporal map reveals dominant expression patterns. *Science* 318(5851):801-806.
16. Winter D*, et al.* (2007) An "Electronic Fluorescent Pictograph" browser for exploring and analyzing large-scale biological data sets. *PLoS One* 2(8):e718.
17. Matsuzaki Y, Ogawa-Ohnishi M, Mori A, & Matsubayashi Y (2010) Secreted peptide signals required for maintenance of root stem cell niche in Arabidopsis. *Science* 329(5995):1065-1067.
18. Li J & Nam KH (2002) Regulation of brassinosteroid signaling by a GSK3/SHAGGY-like kinase. *Science* 295(5558):1299-1301.
19. Noguchi T*, et al.* (1999) Brassinosteroid-insensitive dwarf mutants of Arabidopsis accumulate brassinosteroids. *Plant Physiol* 121(3):743-752.
20. Jaillais Y, Belkhadir Y, Balsemao-Pires E, Dangl JL, & Chory J (2011) Extracellular leucine-rich repeats as a platform for receptor/coreceptor complex formation. *Proc Natl Acad Sci U S A* 108(20):8503-8507.
21. Vragovic K*, et al.* (2015) Translatome analyses capture of opposing tissue-specific brassinosteroid signals orchestrating root meristem differentiation. *Proc Natl Acad Sci U S A* 112(3):923-928.
22. Szekeres M*, et al.* (1996) Brassinosteroids rescue the deficiency of CYP90, a cytochrome P450, controlling cell elongation and de-etiolation in Arabidopsis. *Cell* 85(2):171-182.
23. Kutschmar A*, et al.* (2009) PSK-alpha promotes root growth in Arabidopsis. *New Phytol* 181(4):820-831.
24. Komori R, Amano Y, Ogawa-Ohnishi M, & Matsubayashi Y (2009) Identification of tyrosylprotein sulfotransferase in Arabidopsis. *Proc Natl Acad Sci U S A* 106(35):15067-15072.

Supplemental Figures and Tables

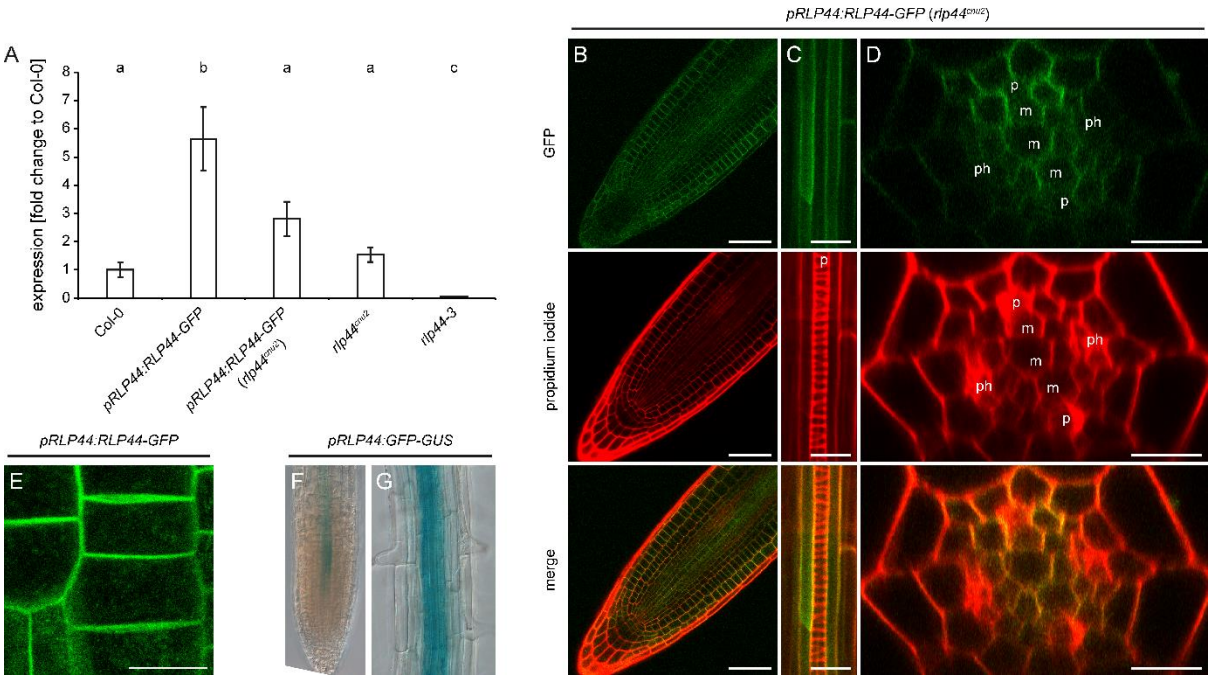

Fig. S1: *RLP44* is expressed in the root vascular tissue. (A) Quantitative Real Time PCR analysis of *RLP44* expression levels in transgenic RLP44-GFP lines and *rlp44* mutants. Note that *rlp44*^{cnu2} carries a point mutation creating a premature stop codon, whereas *rlp44-3* is a T-DNA insertion line (1). Bars denote mean ±SEM of four experiments, letters indicate statistically significant differences based on one-way ANOVA, n = 3. (B) Expression of *RLP44* fused to GFP under control of its own regulatory 5' sequences (*pRLP44:RLP44-GFP*) in the *rlp44*^{cnu2} mutant background. With the exception of the columella, all root meristem cells show GFP fluorescence, but intensity is increased in epidermis, lateral root cap, and vascular precursor cells. Scale bar = 50 µm. (C) Expression of *pRLP44:RLP44-GFP* (*rlp44*^{cnu2}) in differentiating xylem cells. Scale bar = 10 µm. (D) Orthogonal view of a confocal stack recording expression of *pRLP44:RLP44-GFP* in the differentiating vascular tissue of *rlp44*^{cnu2} roots. Note increased fluorescence in procambial cells. Scale bar = 10 µm. Indicated are differentiated phloem (ph), and protoxylem (p), as well as yet undifferentiated metaxylem (m). (E) High magnification image of a root cortex cell expressing pRLP44:RLP44-GFP, showing plasma membrane and intracellular vesicular localization, in agreement with previous observations (1). (F) A reporter line expressing the *uidA* gene under control of the RLP44 promoter displays epidermal and vascular reporter gene activity in the root.

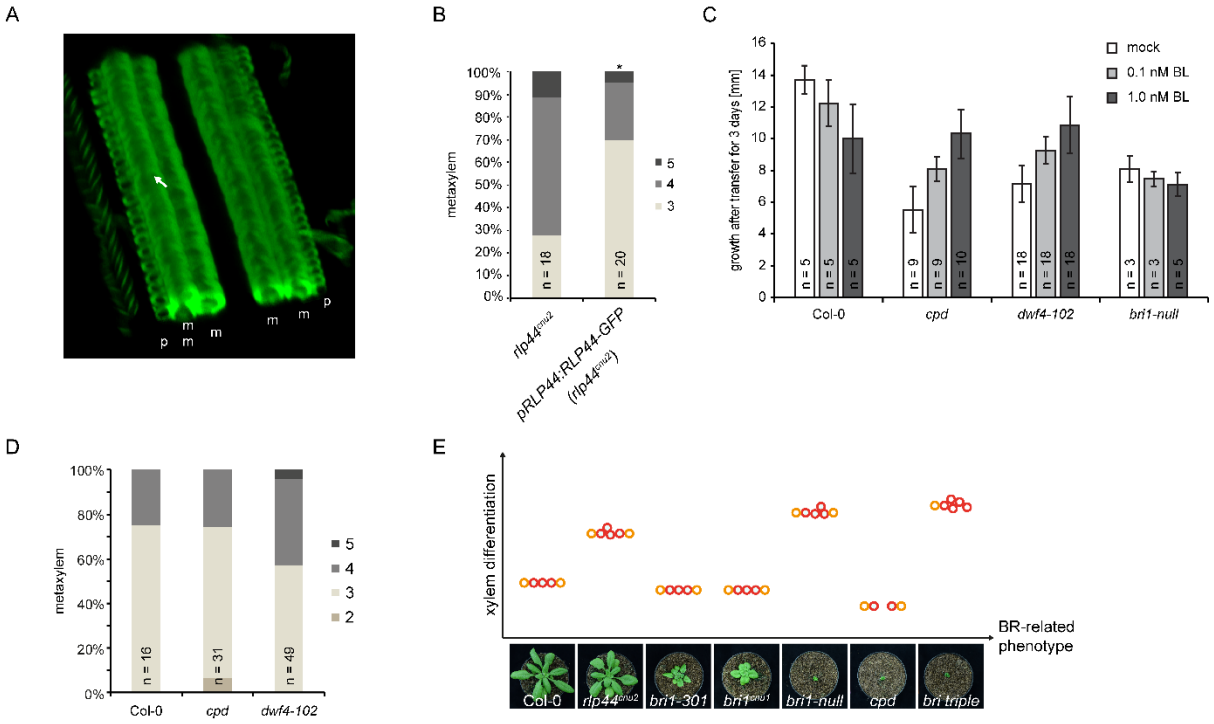

Fig. S2. (A) 3D reconstruction of a stack taken from an *rlp44-3* root indicating ectopic xylem cell (arrow) with pitted metaxylem (m)-like secondary cell wall patterning rather than spiral/annular protoxylem (p) patterning. (B) Expression of *RLP44* under control of its own promoter complements the *rlp44*^{cnu2} xylem phenotype. (C) The BR biosynthetic mutants *cpd* and *dwf4-102* behave similarly in the response to BL, whereas the *bri-null* mutant is insensitive. Bars indicate average growth in mm ± SD after transfer to BL- or DMSO (mock)-containing plates from 4 DAG to 7 DAG. (D) Metaxylem cell number in the *cpd* and *dfw4-102* mutants. (E) Overview over ectopic xylem phenotypes of *rlp44* and BR-related mutants. Note the absence of correlation between severity of BR signalling deficiency (x-axis) and frequency of ectopic xylem phenotype (y-axis). Based on Fig. 2C and D. Bars in (A) and (C) denote frequency of roots with the indicated number of xylem cells. Asterisk indicates statistically significant difference based on Dunn's post-hoc test with Benjamini-Hochberg correction after Kruskal-Wallis modified U-test (*p < 0.05, **p<0.01, ***p<0.001; n.s. = not significant).

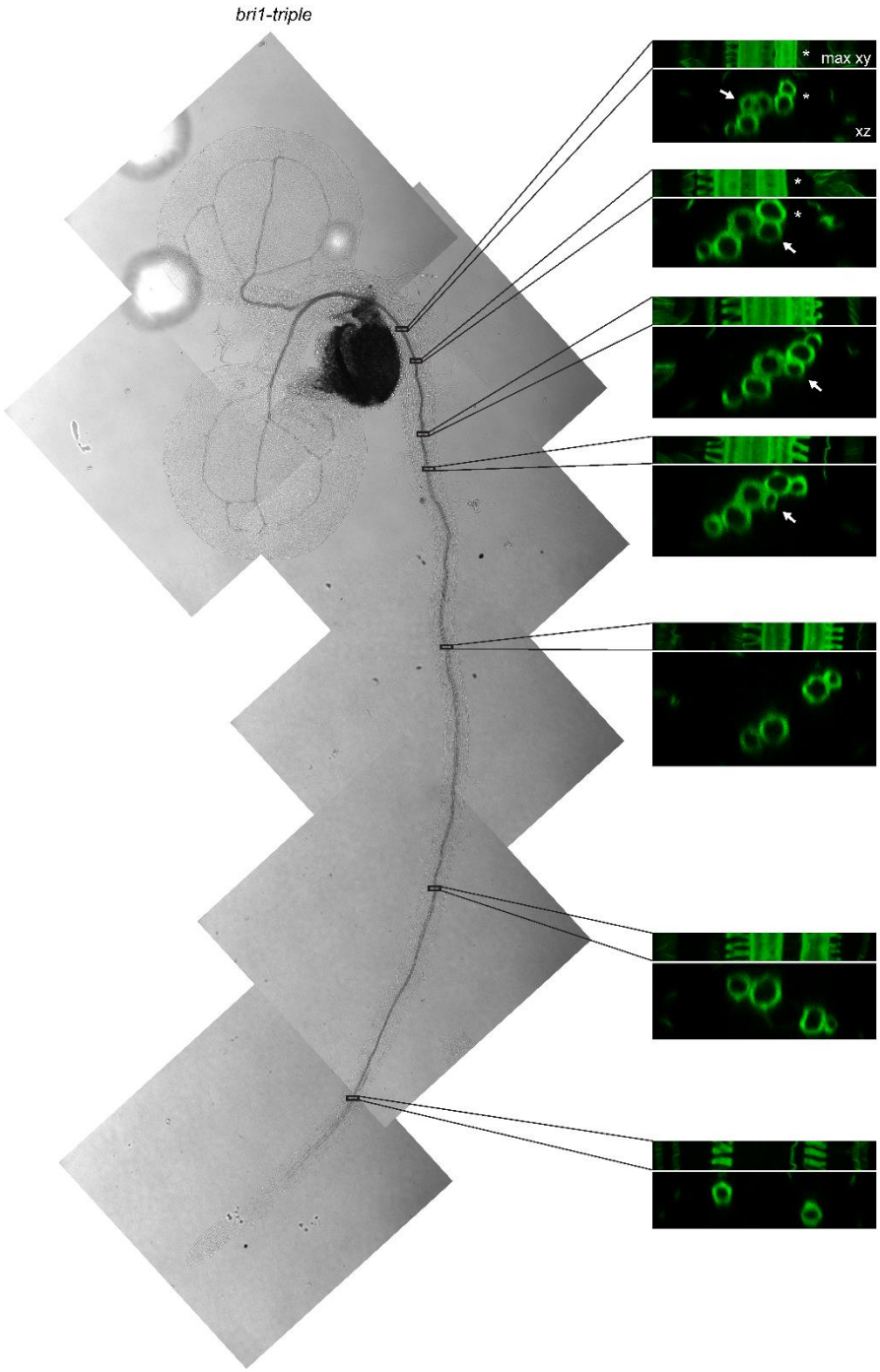

Fig. S3. Overview over xylem phenotype in a 6-day old *bri1-triple* seedling. Approximate imaging position for each stack is indicated. Top Panels are maximum xy projections of the stacks, lower panels show orthogonal xz views. Arrows indicate ectopic metaxylem, asterisks indicate missing protoxylem.

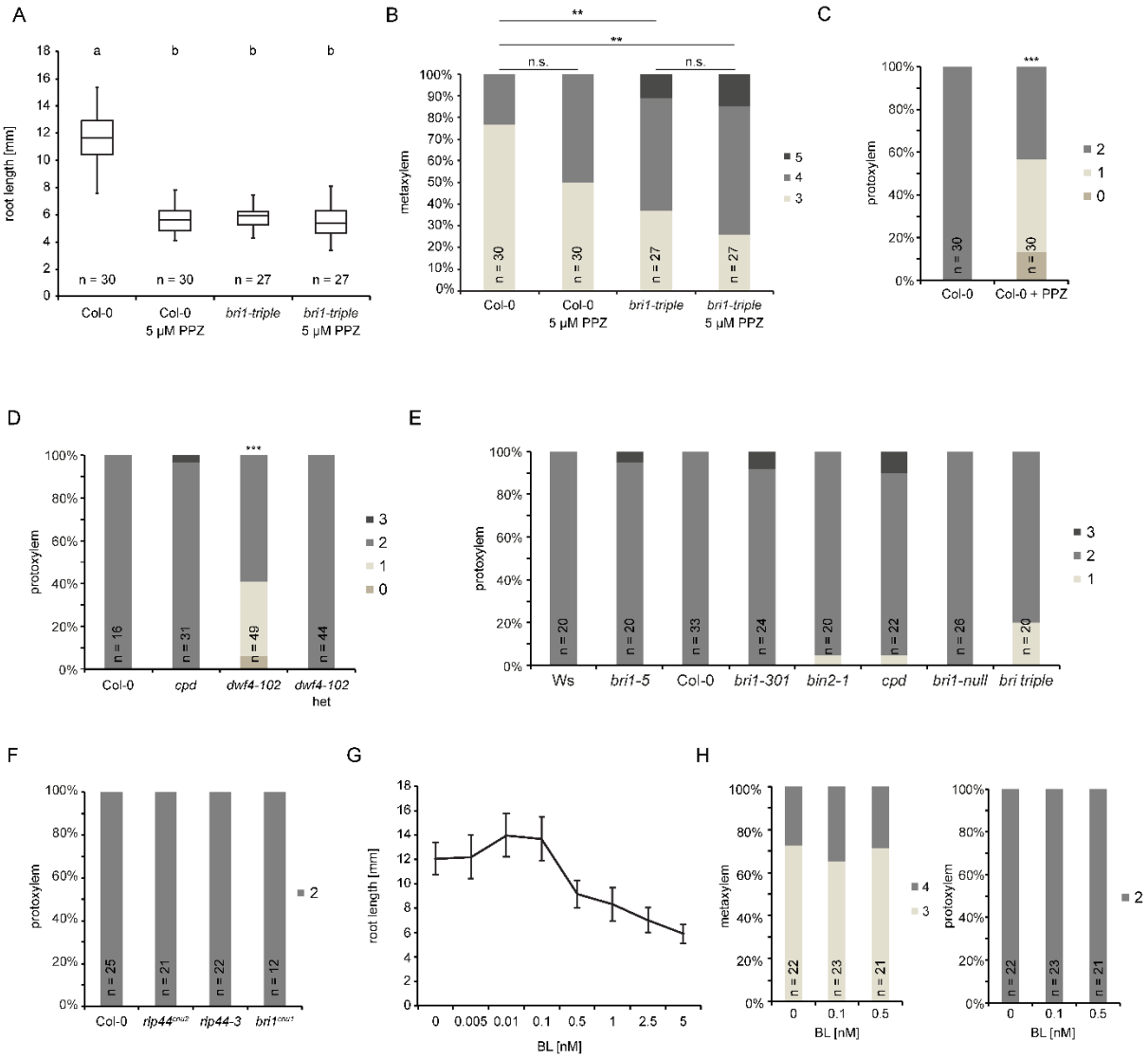

Fig. S4. (A) Depletion of BRs by PPZ treatment leads to *bri-triple*-like growth in the wild type and does not further reduce *bri-triple* root growth. Box plots indicate interquartile range (box), median (bar) and minimum/maximum (whiskers). (B) Metaxylem cell numbers are not significantly altered by depletion of BRs. (C) Depletion of BRs by PPZ treatment results in protoxylem defects. (D) *dwf4-102*, but not *cpd* shows reduced protoxylem cell number. Het = heterozygous and wildtype plants of the segregating *dwf4-102* population (E and F) Protoxylem cell number of genotypes analysed in Fig. 2. (G) Dose-response curve of wildtype root growth in the presence of exogenously supplied BL. (H) Neither a growth promoting, nor a growth inhibiting dose (see (G)) of BL has an effect on metaxylem (left panel) or protoxylem (right panel) cell number. Bars in (B-F, and H) denote frequency of roots with the indicated number of xylem cells. Asterisks indicate statistically significant difference based on Dunn's post-hoc test with Benjamini-Hochberg correction after Kruskal-Wallis modified U-test (**p<0.01, ***p<0.001; n.s. = not significant).

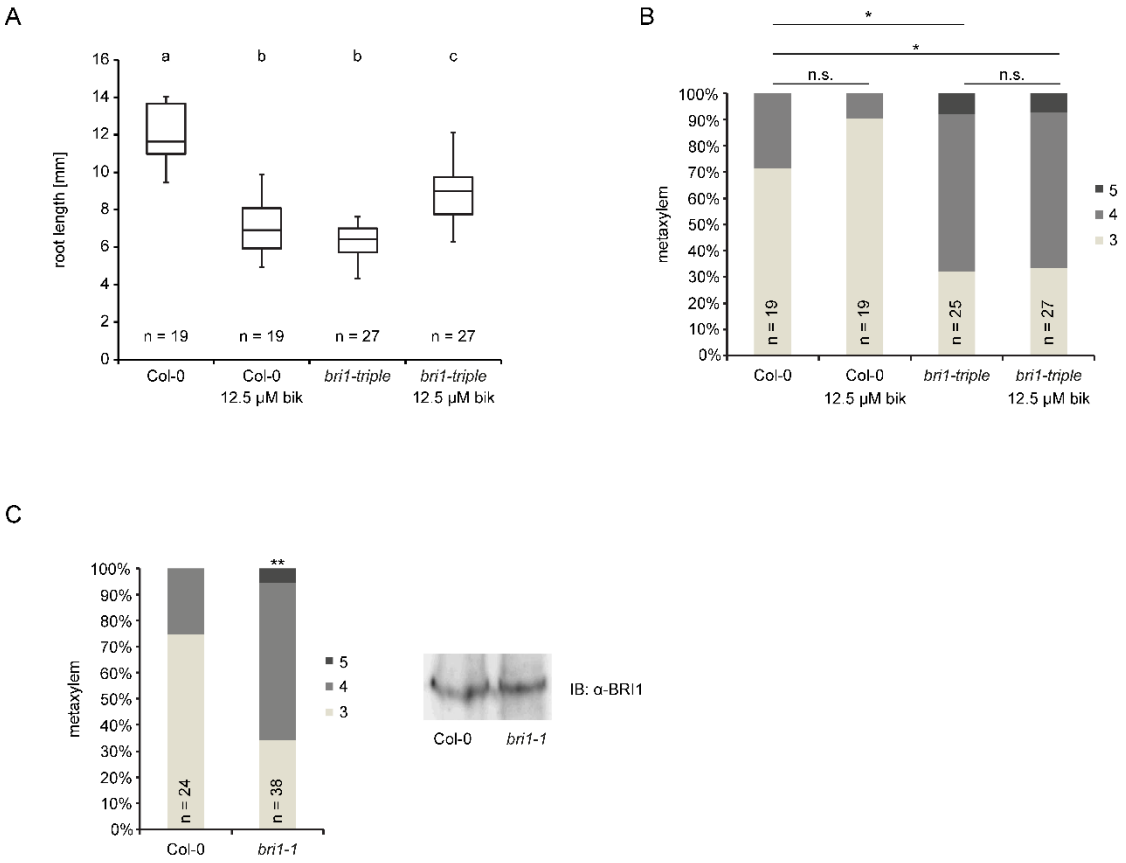

Fig. S5. (A) Root length measurements of Col-0 and *bri-triple* with and without bikinin treatment indicate that 12.5 µM bikinin leads to growth depression in the wildtype, but partially rescues *bri1-triple* root growth. (B) Bikinin treatment has no effect on Col-0 and *bri-triple* metaxylem cell number. (C) Metaxylem cell number is increased in the kinase dead *bri1-1* mutant despite the presence of wild type-like BRI1 protein levels. Left panel shows frequency of metaxylem cell numbers in Col-0 and *bri1-1*, whereas right panel shows a Western Blot developed with antiserum against BRI1 with total protein samples from the same genotypes. Box plots in (A) indicate interquartile range (box), median (bar) and minimum/maximum (whiskers). Bars in (B) and (C) denote frequency of roots with the indicated number of metaxylem cells. Asterisks indicate statistically significant difference based on Dunn's post-hoc test with Benjamini-Hochberg correction after Kruskal-Wallis modified U-test (*$p < 0.05$, **$p<0.01$; n.s. = not significant).

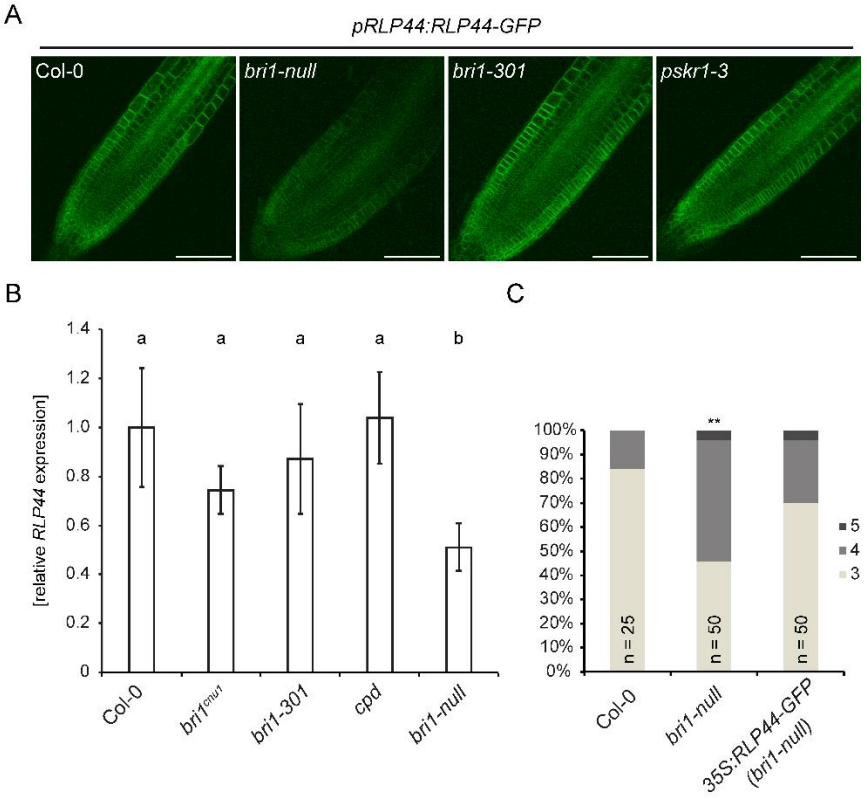

Fig. 6. RLP44 function requires the presence of BRI1 independent of BR signalling strength. (A) Fluorescence intensity derived from RLP44-GFP expressed under control of its own promoter is decreased in the *bri1-null* mutant but largely unaffected in *bri1* hypomorphs and *pskr1-3*. The same *pRLP44:RLP44-GFP* line in Col-0 background was used for crossing with the indicated mutants. (B) QRT-PCR showing reduced steady state levels of RLP44 transcript in roots *of bri1-null*, but not in the biosynthetic mutant *cpd*. Bars denote mean ± SEM of five experiments. Letters indicates statistically significant differences based on one-way ANOVA. (C) Ubiquitous overexpression of *RLP44* rescues the *bri1-null* xylem phenotype. Bars denote frequency of roots with the indicated number of metaxylem cells, asteriska indicate statistically significant difference based on Dunn's post-hoc test with Benjamini-Hochberg correction after Kruskal-Wallis modified U-test **p<0.01).

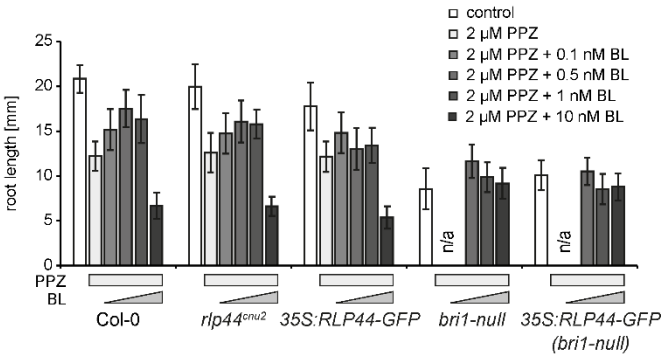

Fig. S7. RLP44 does not promotes BR response *bri1-null*. (A) Response of Col-0, *rlp44*^{cnu2}, *35S:RLP44-GFP*, *bri1-null*, and *35S:RLP44-GFP* (*bri1-null*) to depletion (PPZ) and exogenous supply of brassinosteroids. Bars indicate average root length ± S.D. ($17 < n < 21$). Note that homozygous *bri1-null* mutants are infertile. Therefore, offspring of a heterozygous plant was used and *bri1-null* homozygotes were selected based on phenotype (shorter and thicker root, dark green cotyledons); both genotypes showed the expected 1:3 segregation ratio. Due to the BR deficiency phenotype induced in all plants, PPZ and PPZ + 0.1 nM BL conditions did not allow for confident identification of *bri1-null* mutants.

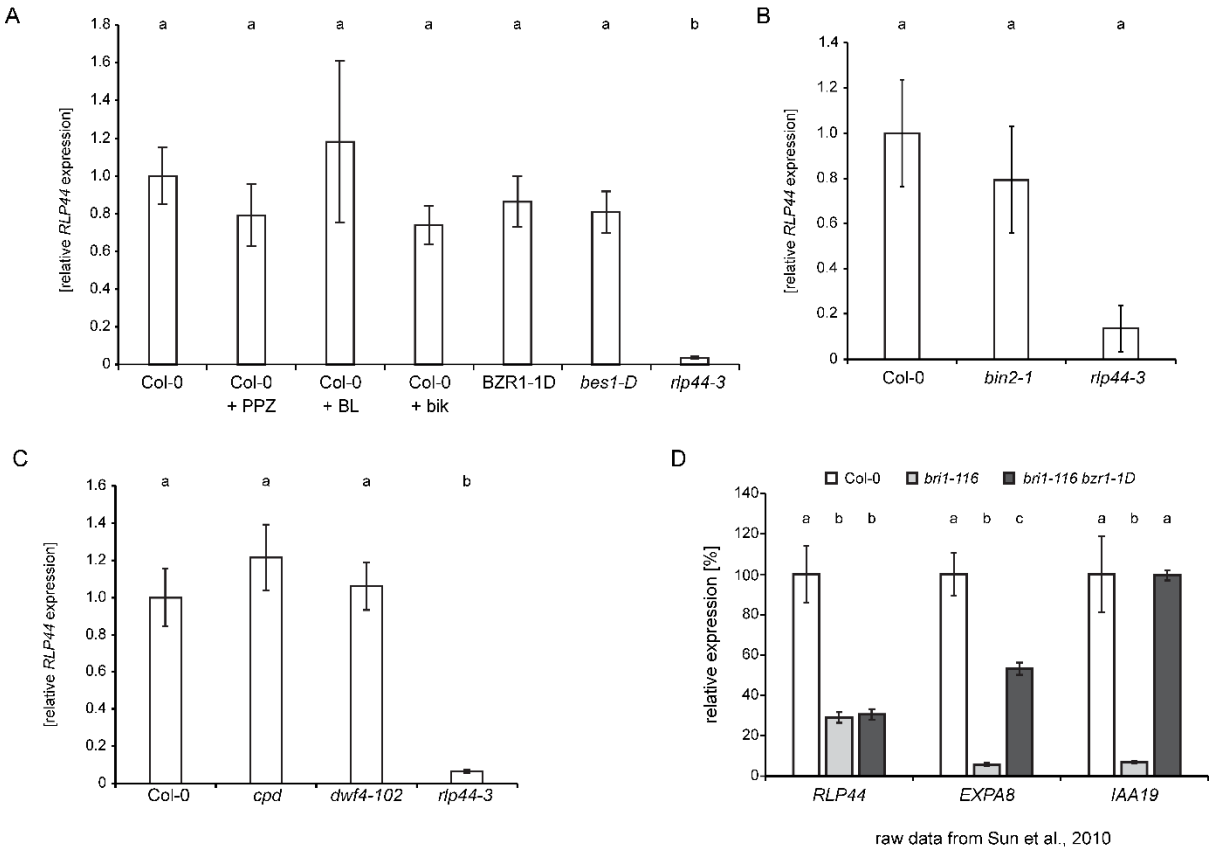

Fig. S8. *RLP44* expression is not affected by BR signalling-related cues. (A-C) QRT-PCR estimation of relative *RLP44* transcript levels upon the indicated treatments and genotypes. Bars denote averages of three biological replicates (two to three technical replicates each) ± SEM. BZR1-1D indicates the *pBZR1:bzr1-1D-CFP* line (12). Letters indicate statistically significant differences based on one-way ANOVA. (D) Re-analysis of published transcriptome data (13) shows that *RLP44* transcript levels are reduced in the null allele *bri1-116* and are not recovered by the constitutively active transcriptions factor *bzr1-1D*, unlike canonical BR target genes such as *EXPA8* and *IAA19*. Bars denote averages of three biological replicates ±SD. Letters indicate statistically significant differences based on one-way ANOVA.

A

Dataset: 21 perturbations from data selection: DATA-AT_AFFY_ATH1-3
Showing 1 measure(s) of 1 gene(s) on selection: AT-0

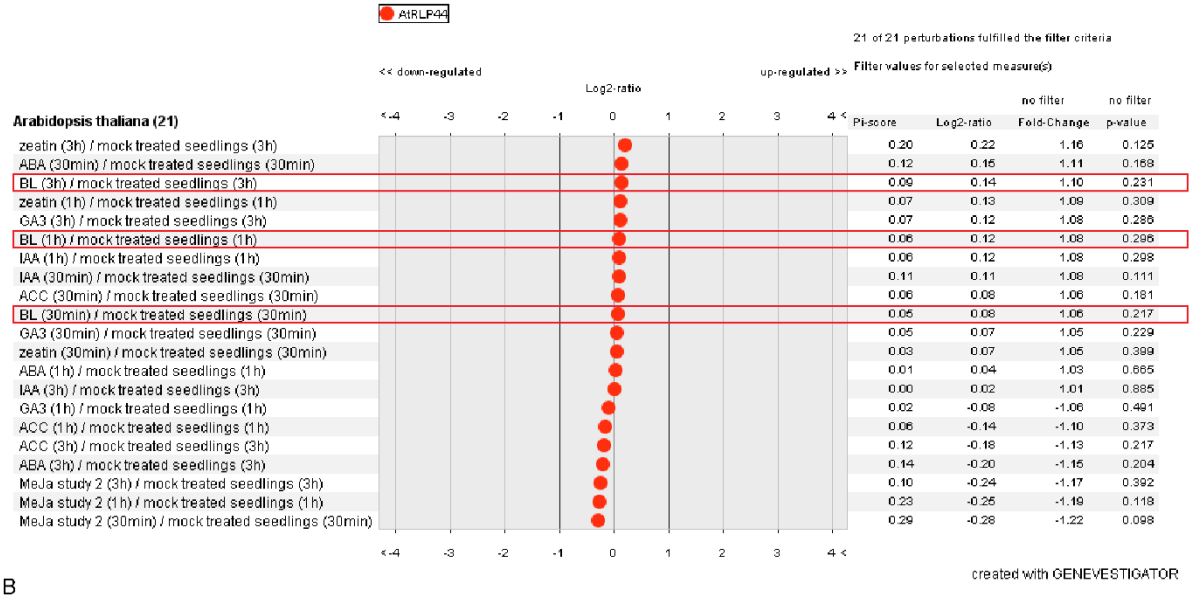

Arabidopsis thaliana (21)	Pi-score	Log2-ratio	no filter Fold-Change	no filter p-value
zeatin (3h) / mock treated seedlings (3h)	0.20	0.22	1.16	0.125
ABA (30min) / mock treated seedlings (30min)	0.12	0.16	1.11	0.168
BL (3h) / mock treated seedlings (3h)	0.09	0.14	1.10	0.231
zeatin (1h) / mock treated seedlings (1h)	0.07	0.13	1.09	0.309
GA3 (3h) / mock treated seedlings (3h)	0.07	0.12	1.08	0.286
BL (1h) / mock treated seedlings (1h)	0.06	0.12	1.08	0.295
IAA (1h) / mock treated seedlings (1h)	0.06	0.12	1.08	0.298
IAA (30min) / mock treated seedlings (30min)	0.11	0.11	1.08	0.111
ACC (30min) / mock treated seedlings (30min)	0.06	0.08	1.06	0.181
BL (30min) / mock treated seedlings (30min)	0.05	0.08	1.06	0.217
GA3 (30min) / mock treated seedlings (30min)	0.05	0.07	1.05	0.229
zeatin (30min) / mock treated seedlings (30min)	0.03	0.07	1.05	0.399
ABA (1h) / mock treated seedlings (1h)	0.01	0.04	1.03	0.665
IAA (3h) / mock treated seedlings (3h)	0.00	0.02	1.01	0.885
GA3 (1h) / mock treated seedlings (1h)	0.02	-0.08	-1.06	0.491
ACC (1h) / mock treated seedlings (1h)	0.06	-0.14	-1.10	0.373
ACC (3h) / mock treated seedlings (3h)	0.12	-0.18	-1.13	0.217
ABA (3h) / mock treated seedlings (3h)	0.14	-0.20	-1.15	0.204
MeJa study 2 (3h) / mock treated seedlings (3h)	0.10	-0.24	-1.17	0.392
MeJa study 2 (1h) / mock treated seedlings (1h)	0.23	-0.25	-1.19	0.118
MeJa study 2 (30min) / mock treated seedlings (30min)	0.29	-0.28	-1.22	0.098

created with GENEVESTIGATOR

B

Dataset: 5 perturbations from data selection: DATA-AT_mRNASeq_ARABI_GL-4
Showing 1 measure(s) of 1 gene(s) on selection: AT-0

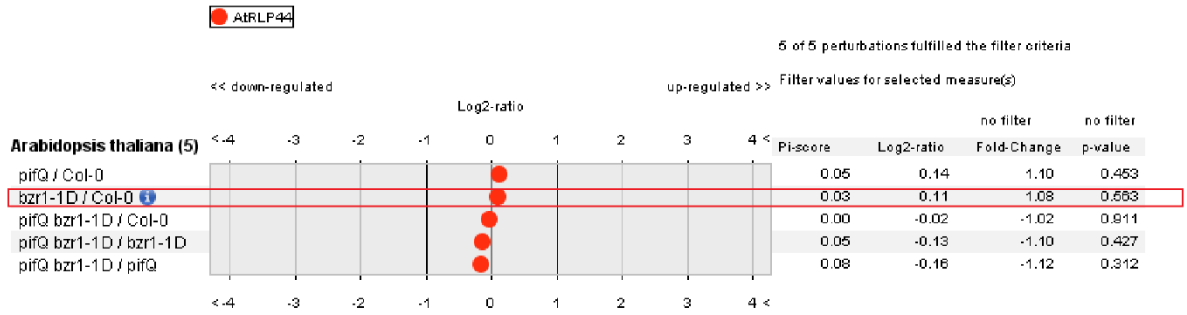

Arabidopsis thaliana (5)	Pi-score	Log2-ratio	no filter Fold-Change	no filter p-value
pifQ / Col-0	0.05	0.14	1.10	0.453
bzr1-1D / Col-0	0.03	0.11	1.08	0.553
pifQ bzr1-1D / Col-0	0.00	-0.02	-1.02	0.911
pifQ bzr1-1D / bzr1-1D	0.05	-0.13	-1.10	0.427
pifQ bzr1-1D / pifQ	0.08	-0.16	-1.12	0.312

created with GENEVESTIGATOR

C

Dataset: 18 perturbations from data selection: DATA-AT_AFFY_ATH1-0
Showing 1 measure(s) of 1 gene(s) on selection: AT-0

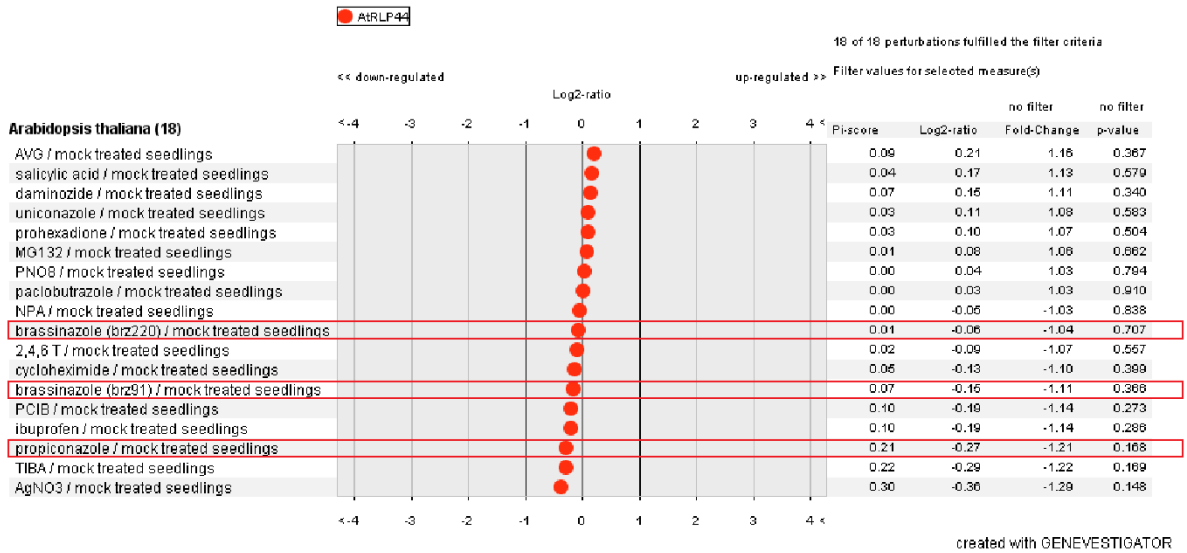

Arabidopsis thaliana (18)	Pi-score	Log2-ratio	no filter Fold-Change	no filter p-value
AVG / mock treated seedlings	0.09	0.21	1.16	0.367
salicylic acid / mock treated seedlings	0.04	0.17	1.13	0.579
daminozide / mock treated seedlings	0.07	0.15	1.11	0.340
uniconazole / mock treated seedlings	0.03	0.11	1.08	0.583
prohexadione / mock treated seedlings	0.03	0.10	1.07	0.504
MG132 / mock treated seedlings	0.01	0.08	1.06	0.662
PNO8 / mock treated seedlings	0.00	0.04	1.03	0.784
paclobutrazole / mock treated seedlings	0.00	0.03	1.03	0.910
NPA / mock treated seedlings	0.00	-0.05	-1.03	0.838
brassinazole (brz220) / mock treated seedlings	0.01	-0.06	-1.04	0.707
2,4,6 T / mock treated seedlings	0.02	-0.09	-1.07	0.557
cycloheximide / mock treated seedlings	0.05	-0.13	-1.10	0.389
brassinazole (brz91) / mock treated seedlings	0.07	-0.15	-1.11	0.366
PCIB / mock treated seedlings	0.10	-0.19	-1.14	0.273
ibuprofen / mock treated seedlings	0.10	-0.19	-1.14	0.286
propiconazole / mock treated seedlings	0.21	-0.27	-1.21	0.168
TIBA / mock treated seedlings	0.22	-0.29	-1.22	0.169
AgNO3 / mock treated seedlings	0.30	-0.36	-1.29	0.148

created with GENEVESTIGATOR

Fig. S9. Publicly available transcriptome datasets (10) suggest limited response of *RLP44* expression to various treatments. BR signalling-related conditions are highlighted.

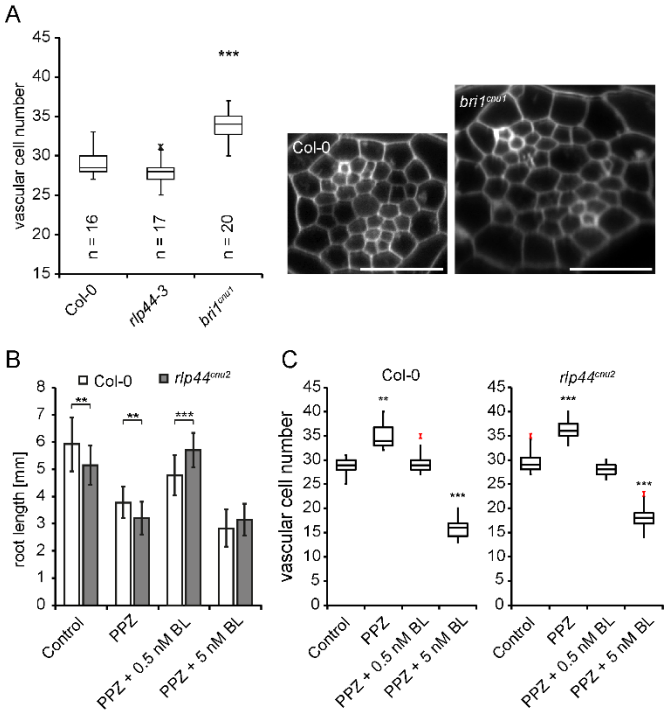

Fig. S10. RLP44 and BRI1 determine vascular cell fate independent of BR signalling-mediated control of cell proliferation. (A) Box-plot quantification of vascular cell number. Asterisks indicate statistically significant difference from Col-0 after pairwise t-test with ***p < 0.001. Optical cross sections of caclofluor white-stained roots were taken in the differentiation zone prior to maturation of the casparian strip. (B) Response of root length to depletion and exogenous addition of brassinosteroids in Col-0 and *rlp44*^{cnu2}. Bars denote mean root length ± SD, n = 14-26. Asterisks denote statistically significant differences after one-way ANOVA and Tukey's post hoc test between Col-0 and *rlp44*^{cnu2} with **p < 0.01 and *** p<0.001. (C) Response of vascular cell number to depletion (PPZ) and exogenous addition of BL in Col-0 and *rlp44*^{cnu2}. Asterisks indicate statistically significant differences from control conditions as determined by two-tailed t test with **p < 0.01 and *** p<0.001. Box plots in (A) and (C) indicate interquartile range (box), median (bar) and minimum/maximum (whiskers).

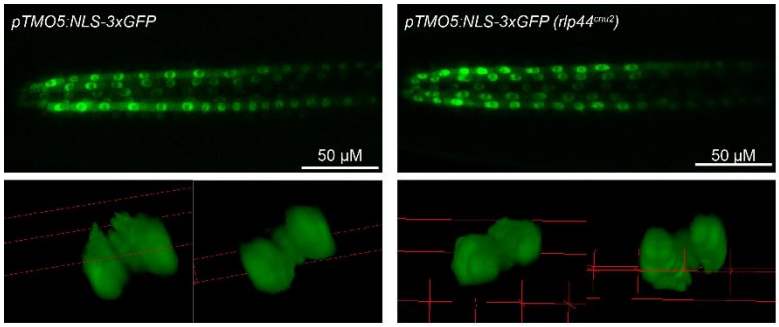

Fig. S11. The expression domain of the xylem precursor marker *pTMO5:NLS-3xGFP* (14) is not altered in *rlp44*^{cnu2} root apical meristems. Upper panels depict median section through root tips showing TMO5-positive cells in the xylem axis. Lower panels depict 3D projections of confocal stacks to visualize absence of TMO5-positive cells outside of the xylem axis.

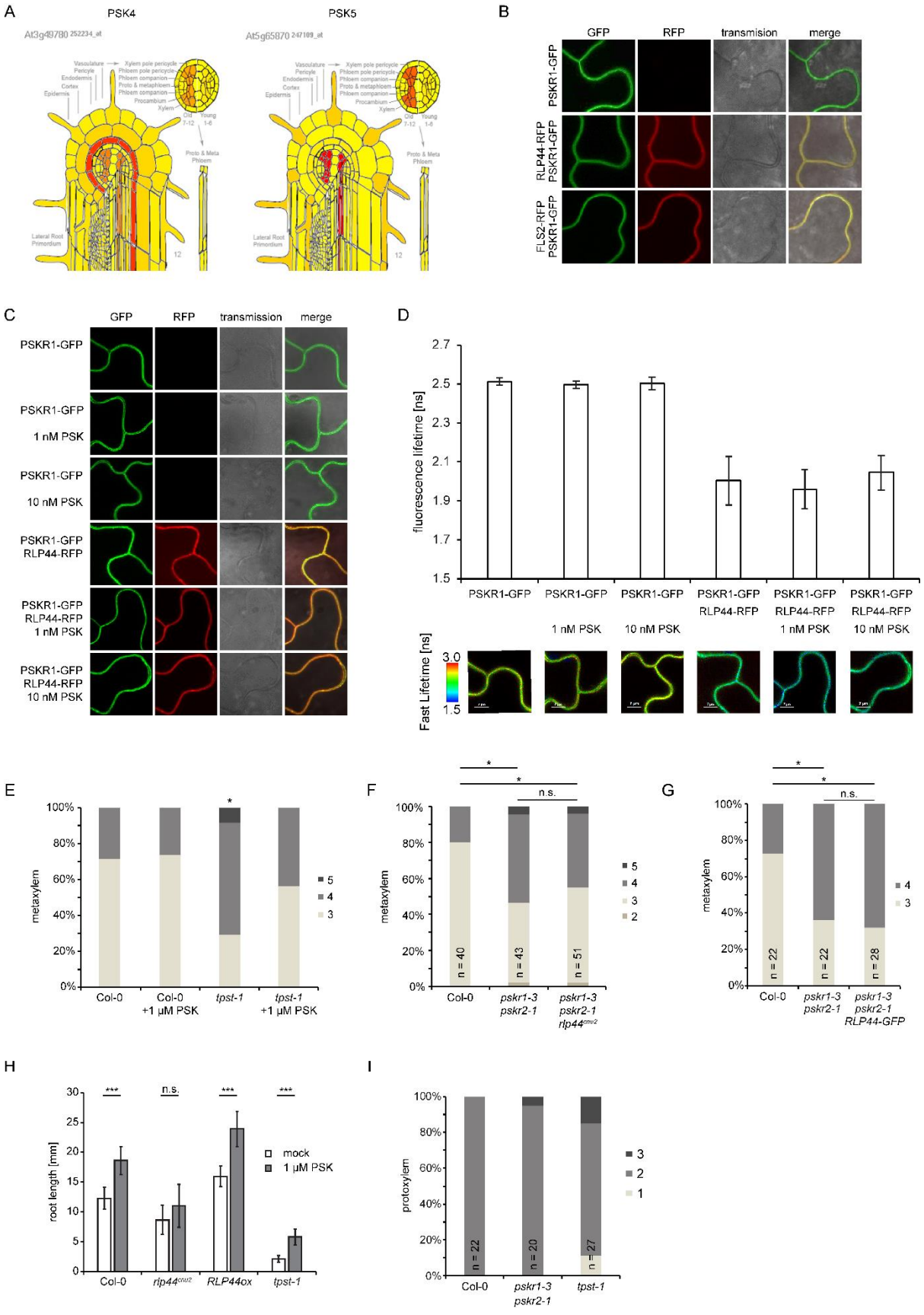

Fig. S12. RLP44 physically and genetically interacts with PSKR1. (A) *PSK* genes are co-expressed with *RLP44* in procambial cells. Tissue-specific expression pattern of *PSK4* and *PSK5* in the root. Data from (15) were analyzed using the eFP browser

(http://bar.utoronto.ca/efp/cgibin/efpWeb.cgi) (16). (B) Representative images of FRET-FLIM experiment analysed in Fig. 3B. (C, D) Interaction of RLP44 and PSKR1 is not modified by exogenous application of PSK. Representative confocal images of *Nicotiana benthamiana* epidermal leaf cells transiently expressing the indicated fusion proteins in the presence or absence of PSK (C) and FRET-FLIM analysis of the RLP44-PSKR1 interaction in the presence or absence of PSK (D) are shown. Bars denote the average of 14 measurements, each ± SD. Micrographs below bars depict fluorescence lifetime heat maps of representative plasma membrane areas used for the FLIM measurements. PSK in the indicated concentrations was applied to the leaf by vacuum infiltration 2 days after *Agrobacterium* transformation. FRET-FLIM measurements were started 15 min after infiltration. Mock treatment was carried out in the identical way but without PSK. (E) Exogenous application of PSK does not alter WT metaxylem cell number, but partially rescues the biosynthetic mutant *tpst-1*. (F) The xylem phenotype in the *pskr1-3 pskr2-1 rlp44*^{cnu2} triple mutant is not enhanced compared to *the pskr1-3 pskr2-1* double mutant. (G) Overexpression of *RLP44* (*p35S:RLP44-GFP*) cannot rescue the *pskr1-3 pskr2-1* mutant. (H) The *rlp44*^{cnu2} mutant is quantitatively challenged in the root growth response to PSK. The growth phenotype of *tpst-1* is only partially rescued by the treatment, in agreement with published data (17), as full recovery requires co-treatment with the sulfated peptide ROOT GROWTH FACTOR1. (I) PSK-related mutants do not show pronounced reduction in protoxylem cell numbers. Bars in (E—G, and I) denote frequency of roots with the indicated number of xylem cells. Asterisk indicates statistically significant difference based on Dunn's post-hoc test with Benjamini-Hochberg correction after Kruskal-Wallis modified U-test (*$p < 0.05$). n.s. = not significant.

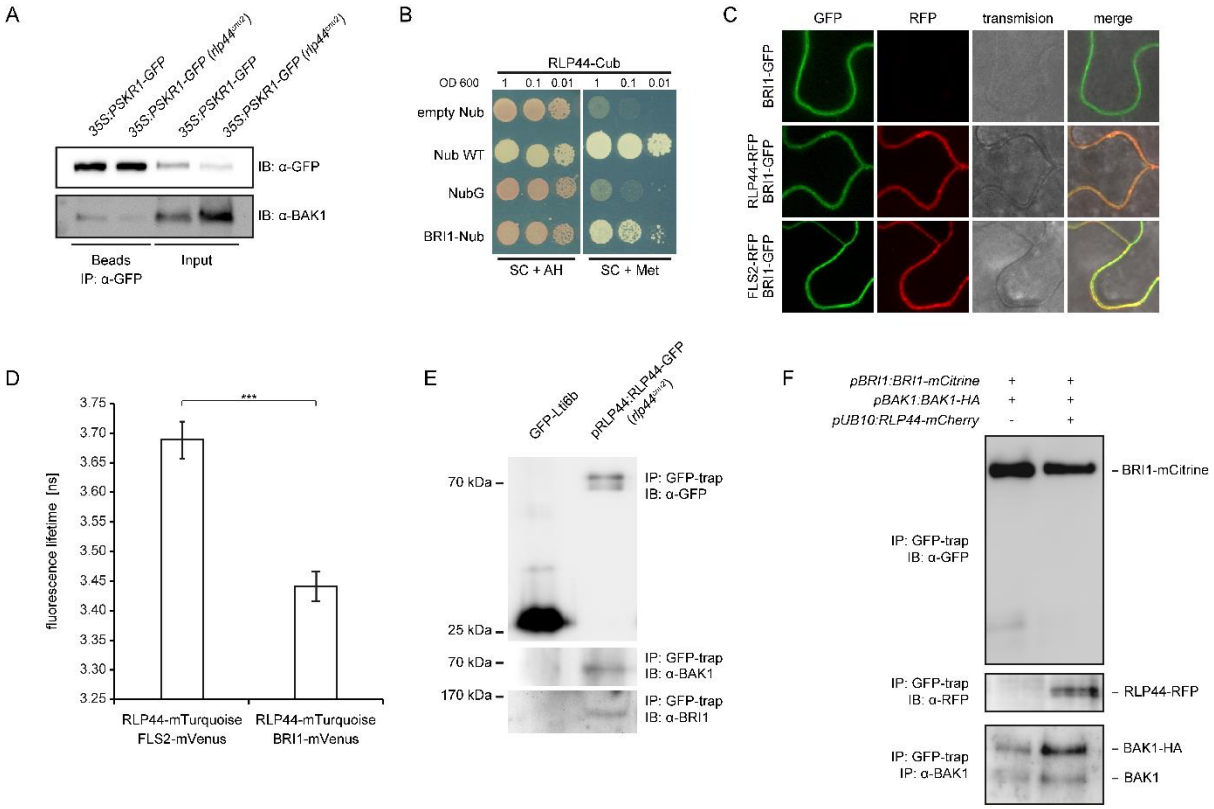

Fig. S13. BRI1 directly interacts with RLP44. (A) Mating-based split-Ubiquitin analysis in yeast reveals direct interaction of RLP44 and BRI1. After mating, presence of RLP44-Cub and BRI1-Nub enables yeast growth under selective conditions (SC + Met). Empty Nub vector and NubG are used as negative controls whereas interaction with WT Nub serves as a positive control. (B) FRET-FLIM analysis of RLP44-mTurquoise and BRI1-mVenus interaction. The related LRR-RLK FLS2 is used as a negative control. Bars indicate mean fluorescence lifetime ± SD (n = 11), asterisks indicate statistical significance according to two-tailed t test with ***p > 0.001. (C) RLP44 is present in BRI1 and BAK1 containing complexes under native expression levels. Immunoprecipitates of RLP44-GFP expressed under control of its own promoter in the *rlp44*^{cnu2} background were probed with antisera raised against BRI1 and BAK1 (6). (D) Presence of RLP44 enhances interaction between BRI1 and BAK1 in a line expressing BRI1-mCitrine and BAK1-HA from their native promoters in the *bri1-null* mutant background.

Table S1: Mutants and transgenic lines used in this study

Mutant/transgenic line	Reference	Acession
rlp44^{cnu2}	(1)	
rlp44-3	(1)	SAIL_596_E12
bri1^{cnu1}	(11)	
bri1-301	(18)	
bri1-5	(19)	
bri1-null	(20)	GK-134E10
bri1-1	(Clouse 1996; Friedrichsen et al., 2000)	
bri triple	(21)	*bri1-116*; SALK_005982 (*brl1*); SALK_006024 (*brl3*)
bin2-1	(18)	
cpd	(22)	
dwf4-102	(Nakamoto et al., 2006)	SALK_020761
pskr1-3 pskr2-1	(23)	
pskr1-3 psy1r1	(24)	
tpst-1	(17)	
pRLP44:RLP44-GFP	This study	
pRLP44:RLP44-GFP (*rlp44*^{cnu2})	This study	
pRLP44:RLP44-GFP (*bri1-301*)	This study	
pRLP44:RLP44-GFP (*bri1-null*)	This study	
pRLP44:RLP44-GFP (*pskr1-3*)	This study	
35S:RLP44-GFP	(1)	
RLP44ox (35S:RLP44-RFP)	(1)	
35S:RLP44-GFP (bri1-null)	This study	
35S:PSKR1-GFP	(23)	
35S:PSKR1-GFP (rlp44^{cnu2}*)*	This study	
pBRI1:BRI1-GFP (bri1-null)	This study	
pRLP44:GFP-GUS	This study	
pTMO5:NLS-3xGFP	(Schlereth et al. 2010)	
pTMO5:NLS-3xGFP (rlp44^{cnu2}*)*	This study	
pBRI1:BRI1-mCitrine/pBAK1:BAK1:HA (bri1-null)	provided by M.Hothorn	GK-134E10
pBRI1:BRI1-mCitrine/pBAK1:BAK1:HA(pUBQ10:RLP44-mCherry (bri1-null)	This study	GK-134E10

Table S2: Oligonucleotides used in this study

Oligonucleotide	Sequence
BRI1_3'UTR_R	aaacgaaaacattacaaatcc
BRI1-GK_WT_F	AACTATGGCTGAATATGTTAG
GK-o8409	ATATTGACCATCATACTCATTGC
BRI1_ GK-134E10_R	TCGTTCCATTGAAGAGATTGG
RLP44prom_GW_L	GGGGACAAGTTTGTACAAAAAAGCAGGCTtttgcgatatttttggctgtc
RLP44prom_GW_R	GGGGACCACTTTGTACAAGAAAGCTGGGTttttaaattttagagaggtttc
FLS2_attB1_F	GGGGACAAGTTTGTACAAAAAAGCAGGCTATGAAGTTACTCTCAA AGAC
FLS2_attB4_R	GGGGACAACTTTGTATAGAAAAGTTGGGTGtAACTTCTCGATCCT CGTTACG
RLP44_attb2_R	GGGGACCACTTTGTACAAGAAAGCTGGGTtGTAATCAGGCATAGA TTGAC
RLP44_attb3_F	GGGGACAACTTTGTATAATAAAGTTGATGACAAGGAGTCACCGGT TAC
BRI1_attB2_R	GGGACCACTTTGTACAAGAAAGCTGGGTtTAATTTTCCTTCAGGAA CTTCTT
BRI1_attB3_F	GGGGACAACTTTGTATAATAAAGTTGATGAAGACTTTTTCAAGCTT CTT
BRI1_GGC_1F	AACAGGTCTCAGGCTCATGAAGACTTTTTCAAGCTTCT
BRI1_GGC_1R	AACAGGTCTCaATCACACGCGCCGGAGAGAAAGTCAG
BRI1_GGC_2F	aacaGGTCTCaTGATACACTCACTGGaCTCGATCTCTCTGGA
BRI1_GGC_2R	aacaGGTCTCaGAGtCCAGGATTGTTCAAGAA
BRI1_GGC_3F	aacaGGTCTCaACTCTGTGGTTATCCTCTT
BRI1_GGC_3R	aacaggTCTCaGGCCTCCTTCCATGAGATCT
BRI1_GGC_4F	aacaGGTCTCaGgCCAGCGTCCCTTGCTGGT
BRI1_GGC_4R	AACAGGTCTCACTGATAATTTTCCTTCAGGAACTTC
at5G46630_cod_F	TCGATTGCTTGGTTTGGAAGAT
at5G46630_cod_R	GCACTTAGCGTGGACTCTGTTTGC
RLP44_cod2_F	TCAGATTCCGCAGCAATTAG
RLP44_cod2_R	TCCTGCAACGGATAACCATA
SALK_008585_F	CTCGCTTTCTGGTATGACGAG
SALK_008585_R	TCCGAAACTATACACATCGCC
SALK_203857_F	TTCTTAGACTGTTTGGCTCGG
SALK_203857_R	GCGTTACAAACATGCAACAAG
LBb1.3	ATTTTGCCGATTTCGGAAC

Table S3. Overview of constructs generated with GreenGate cloning (Lampropoulos et al., 2013) and the primers used to generate modules, where appropriate.

pSW362	**pRLP44:RLP44-GFP**		
pSW299	RLP44 (at3g49750) promoter	AACAGGTCT**C**AACCTtttgcgatatttttggctgtc	AACAGGTCTCATGTTttttaaattttagagaggtttc
pGGB003	B-Dummy	Lampropoulos et al., 2013	
pSW334	RLP44 (at3g49750) CDS	AACAGGTCTCAGGCTCAATGACAAGGAGTCACCGGTTA	AACAGGTCTCACTGAGTAATCAGGCATAGATTGAC
pGGD001	GFP	Lampropoulos et al., 2013	
pGGE009	UBQ10 terminator	Lampropoulos et al., 2013	
pGGF001	pMAS::BastaR::tMAS	Lampropoulos et al., 2013	
pGGZ0001	destination vector	Lampropoulos et al., 2013	

pSW420	**pBRI1:BRI1-GFP**		
pSW379	BRI1(AT4G39400) promoter	AACAGGTCTCAACCTgatcttccttctttatttg	AACAGGTCTCATGTTttctcaagagtttgtgagag
pGGB003	B-Dummy	Lampropoulos et al., 2013	
pSW380	BRI1(AT4G39400) CDS	AACAGGTCTCAGGCTCATGAAGACTTTTTCAAGCTTC	AACAGGTCTCACTGATAATTTTCCTTCAGGAACTTC
pGGD001	GFP	Lampropoulos et al., 2013	
pGGE009	UBQ10 terminator	Lampropoulos et al., 2013	
pGGF001	pMAS::BastaR::tMAS	Lampropoulos et al., 2013	
pGGZ001	destination vector	Lampropoulos et al., 2013	

pSW375	**pUBQ10:RLP44-mCherry**		
pGGA006	UBQ10 (At4g05320)		
pGGB003	B-Dummy	Lampropoulos et al., 2013	
pSW334	RLP44 (at3g49750) CDS	AACAGGTCTCAGGCTCAATGACAAGGAGTCACCGGTTA	AACAGGTCTCACTGAGTAATCAGGCATAGATTGAC
pGGD003	Linker mCherry	Lampropoulos et al., 2013	
pGGE009	UBQ10 terminator	Lampropoulos et al., 2013	
pGGF005	pUBQ10::HygR::tOCS	Lampropoulos et al., 2013	
pGGZ001	destination vector	Lampropoulos et al., 2013	